Activation of the hypoxia-inducible factor-1α pathway accelerates bone regeneration

Chao Wan*, Shawn R. Gilbert†, Ying Wang*, Xuemei Cao*, Xing Shen*, Girish Ramaswamy‡, Kimberly A. Jacobsen§, Zainab S. Alaql§, Alan W. Eberhardt‡, Louis C. Gerstenfeld§, Thomas A. Einhorn§, Lianfu Deng*, and Thomas L. Clemens*¶‖

Departments of *Pathology, †Surgery, and ‡Biomedical Engineering, University of Alabama at Birmingham, Birmingham, AL 35294; §Department of Orthopaedic Surgery, Boston University Medical Center, Boston, MA 02118; and ¶Veterans Administration Medical Center, Birmingham, AL 35294

Edited by John T. Potts, Jr., Massachusetts General Hospital, Charlestown, MA, and approved November 20, 2007 (received for review September 13, 2007)

The hypoxia-inducible factor-1α (HIF-1α) pathway is the central regulator of adaptive responses to low oxygen availability and is required for normal skeletal development. Here, we demonstrate that the HIF-1α pathway is activated during bone repair and can be manipulated genetically and pharmacologically to improve skeletal healing. Mice lacking *pVHL* in osteoblasts with constitutive HIF-1α activation in osteoblasts had markedly increased vascularity and produced more bone in response to distraction osteogenesis, whereas mice lacking *HIF-1α* in osteoblasts had impaired angiogenesis and bone healing. The increased vascularity and bone regeneration in the pVHL mutants were VEGF dependent and eliminated by concomitant administration of VEGF receptor antibodies. Small-molecule inhibitors of HIF prolyl hydroxylation stabilized HIF/VEGF production and increased angiogenesis *in vitro*. One of these molecules (DFO) administered *in vivo* into the distraction gap increased angiogenesis and markedly improved bone regeneration. These results identify the HIF-1α pathway as a critical mediator of neoangiogenesis required for skeletal regeneration and suggest the application of HIF activators as therapies to improve bone healing.

von Hippel–Lindau protein | VEGF | angiogenesis | distraction osteogenesis

Bone has a unique ability to regenerate and repair itself postnatally. However, of the 6 million fractures reported annually in the United States, as many as 10% have impaired healing. This results in enormous direct and indirect cost to the individual and to society (1). A hallmark of impaired healing in humans and animals is a reduction in vascular supply and nutrient availability at the site of injury, suggesting that impaired angiogenic response is a major contributor to the pathology.

Bone regeneration recapitulates processes that operate during skeletal development and require close temporal and spatial coordination of events involving resident bone cells, marrow stromal elements, and associated vascular structures (2, 3). Angiogenesis is critical for bone regeneration and depends on hypoxic stimuli and VEGF production. The hypoxia-inducible factor (HIF) pathway is the central pathway for sensing and responding to changes in local oxygen availability in a wide variety of organisms. HIF impinges on gene programs that influence angiogenesis (e.g., *VEGF*, *angiopoietins*) and cellular metabolism (*glucose transporter*). In addition, HIF can recruit inflammatory and mesenchymal cells and influence cell differentiation (4–7). Consequently, the HIF pathway is ideally suited to coordinate tissue response to injury.

HIF-1α levels are controlled by regulated proteolysis through an oxygen-sensitive mechanism. Under normoxic conditions, HIF-1α undergoes prolyl hydroxylation and is ligated by von Hippel–Lindau protein (pVHL), an E3 ubiquitin ligase (8–10), and then degraded by the proteosome. The prolyl hydroxylases require iron, 2-oxoglutarate, and oxygen as cofactors (11). Under hypoxia, HIF-1α prolyl hydroxylation is inhibited, and HIF-1α accumulates in the nucleus where it forms a dimer with the HIF-1β subunit (also known as aryl hydrocabon receptor nuclear translocator). The dimer then complexes with coactivator p300 and transactivates HIF responsive genes (12).

We have recently identified the importance of the HIF pathway in skeletal development (13). Mice lacking HIF-1α in osteoblasts were found to have decreased bone volume, whereas targeted deletion of pVHL resulting in increased HIF activation in osteoblasts significantly increased bone volume with a striking increase in bone vascularity. We therefore hypothesized that activation of HIF would increase vascularity and, subsequently, improve bone healing. In this study, we used both genetic and pharmacologic approaches to activate HIF in the mouse distraction osteogenesis (DO) model of skeletal repair that depends highly on neoangiogenesis. Our results demonstrate the requirement of the HIF-1 pathway for mediating the angiogenic and osteogenic phases of bone repair and suggest the feasibility of molecular targeting of the HIF pathway to enhance bone regeneration.

Results

Development of Hypoxia and Expression of HIF-1α Pathway Components During DO. Histological analysis was performed in tissues harvested from 8-week-old male C57BL/6 mice subjected to DO (14). After osteotomy, no manipulation was performed for 7 days of latency. After subsequent distraction over 10 days, new bone formation was apparent in the distraction gap at day 17 and healing was complete by day 38 [supporting information (SI) Fig. 6*A*]. Pimonidazole adducts immunostaining was used to assess tissue hypoxia in the distraction gap after 1 day of distraction. Cells that exhibited morphological features consistent with osteoblasts in the central region of the distraction gap were intensely stained with the antibody to the protein-pimonidazole adducts (SI Fig. 6*B*). HIF-1α and VEGF were also localized to these cells by *in situ* hybridization and immunohistochemistry (SI Fig. 6*C*). Within this region, new blood vessels developed during the distraction phase as assessed by immunohistochemistry for the endothelial marker CD31 (SI Fig. 6*C*) at day 17. These results demonstrate the development of hypoxia in bone lining cells during distraction in association with neoangiogenesis and the appearance of HIF-1α and VEGF.

Genetic Activation of the HIF-1α Pathway Promotes Angiogenesis and Enhances Bone Regeneration. We developed two mutant mouse models to investigate the function of HIFs in bone regeneration

Author contributions: C.W. and S.R.G. contributed equally to this work; C.W., S.R.G., and T.L.C. designed research; C.W., S.R.G., Y.W., X.C., X.S., G.R., K.A.J., Z.S.A., and L.D. performed research; C.W., S.R.G., A.W.E., L.C.G., T.A.E., and T.L.C. analyzed data; and C.W., S.R.G., and T.L.C. wrote the paper.

The authors declare no conflict of interest.

This article is a PNAS Direct Submission.

‖To whom correspondence should be addressed at: Department of Pathology, Division of Molecular and Cellular Pathology, University of Alabama, Volker Hall, G001, 1670 University Boulevard, Birmingham, AL 35294-0019. E-mail: tclemens@uab.edu.

This article contains supporting information online at www.pnas.org/cgi/content/full/0708474105/DC1.

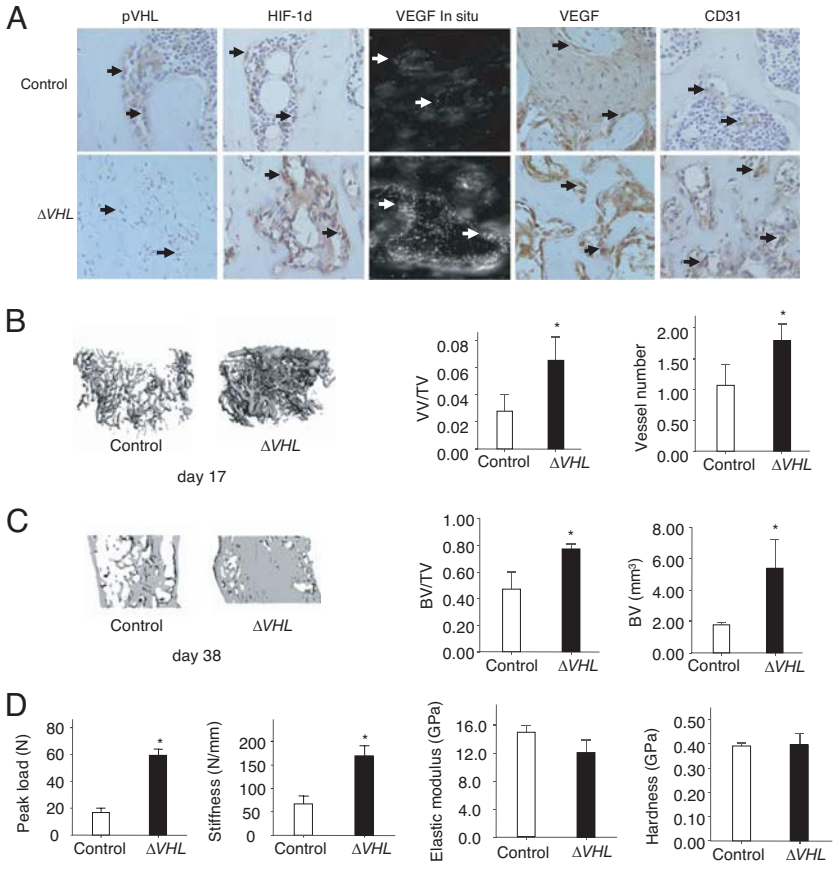

Fig. 1. Genetic activation of the HIF-1α pathway increases neoangiogenesis and promotes bone regeneration. (*A*) Eight-week-old Δ*VHL* mice and control littermates were subjected to DO. Tissues were harvested at day 31 after surgery, and histological sections of the distraction gap were prepared. Representative sections from the Δ*VHL* mice and controls are shown after staining with antibodies against pVHL and HIF-1α. VEGF mRNA expression in bone-lining cells is shown by *in situ* hybridization and immunostaining; CD31 immunostaining is also shown. Arrows show positive cells. (*B*) Representative μCT images of vasculature in Microfil-perfused distraction area from control and the Δ*VHL* mice at day 17 after surgery. Quantitative measurements of vessel volume per total volume (VV/TV) and vessel number are shown. Data represent mean ± SD. *, $P < 0.05$. (*C*) Representative μCT images of distraction area from control and the Δ*VHL* mice at day 38 after surgery. Quantitative measurements of BV and BV/TV are shown. Data represent mean ± SD. *, $P < 0.05$. (*D*) Three-point bending tests (peak load and stiffness) and nanoindentation (elastic modulus and hardness) were performed on tibiae from the Δ*VHL* mice and controls at day 38 after surgery. Data shown represent mean ± SD. *, $P < 0.05$.

during DO. In the first model, we overexpressed HIFs in osteoblasts by disrupting the HIF E-3 ligase, pVHL. As expected, loss of pVHL (Fig. 1*A*) was accompanied by increased HIF-1α protein, increased VEGF mRNA, and protein and increased CD31 immunostaining. To quantify the subsequent angiogenic response, we performed micro computed tomography (μCT) angiography using Microfil at day 17. This time point corresponds to the end of active distraction, when much of the observed angiogenesis and increased blood flow has taken place in DO (15, 16). Increased vascularity was noted in the mutant (Δ*VHL*) mice (Fig. 1*B*). Significant increases in both vessel volume per total volume (VV/TV) and vessel number were observed in the mutants compared with controls (Fig. 1*B*). The Δ*VHL* mice subsequently generated more dense woven bone in the distraction gap compared with controls (Fig. 1*C* and SI Fig. 7). μCT measurements showed significantly increased bone volume (BV) and bone volume per total volume (BV/TV) at days 31 and 38 in the Δ*VHL* mice compared with controls (Fig. 1*C* and SI Fig. 8). Thus, the increased vascularity observed in the Δ*VHL* mice at the conclusion of DO was followed by increased bone formation. Biomechanical testing of the bones by three-point bending showed that peak load and stiffness were significantly increased in Δ*VHL* mice compared with controls (Fig. 1*D*). Nanoindentation showed no significant difference in elastic modulus and hardness between the mutants and controls (Fig. 1*D*). Thus, the increased bone formation in the Δ*VHL* mice led to an increase in structural integrity by increased bone volume with no difference in the material properties of the newly formed bone. Collectively, these results show that genetic activation of the HIF pathway in the Δ*VHL* mice increases angiogenesis and bone regeneration.

VEGF Receptor Antibodies Inhibit Angiogenesis During DO. To determine the importance of VEGF signaling in the enhanced angiogenic response during bone regeneration in the Δ*VHL* mice, we administered VEGFR1 and VEGFR2 antibodies or nonimmune IgG i.p. every 3 days after surgery until day 17. μCT angiography showed that mice given VEGF receptor antibodies had significantly decreased VV/TV, vessel number, and vessel surface with significantly increased vessel separation (Fig. 2 *A* and *B*). These results suggest that the enhanced response to DO seen in the Δ*VHL* mice requires VEGF.

Inactivation of HIF-1α Impairs Angiogenesis and Bone Regeneration. We next examined whether inhibiting HIF-1α would impair angiogenesis and bone healing. We developed a second mouse strain with a targeted deletion of HIF-1α in osteoblasts and subjected them to DO. μCT angiography at day 17 showed decreased vascularity in the Δ*HIF-1α* mice with significant decreases in VV/TV and vessel number compared with controls (Fig. 3*A*). μCT analysis at day 31 demonstrated that subsequent bone regeneration was decreased in Δ*HIF-1α* mice compared with controls, as evidenced by a smaller volume of regenerate in the distraction gap (Fig. 3*B*). These results indicate that HIF-1α is required for normal angiogenesis and bone healing.

Pharmacological Activation of the HIF-1α Pathway Stimulates Angiogenesis and Accelerates Bone Regeneration. A family of oxygen-sensitive prolyl hydroxylases (PHD1,2,3) hydroxylate HIFs under normoxia, which promotes their subsequent E-3 ligation and proteosomal destruction. To identify HIF activators, we tested several agents known to inhibit prolyl hydroxylases for their ability to activate a *HIF*-responsive reporter gene stably expressed in an osteoblast-like osteosarcoma cell line. Desferrioxamine (DFO) and L-mimosine (L-mim) strongly activated the reporter gene expression (Fig. 4*A*). To evaluate the effects of these agents on bone progenitors, we examined *HIF-1α* and *VEGF* expression in primary mouse bone marrow mesenchymal stromal cells (MSCs). Treat-

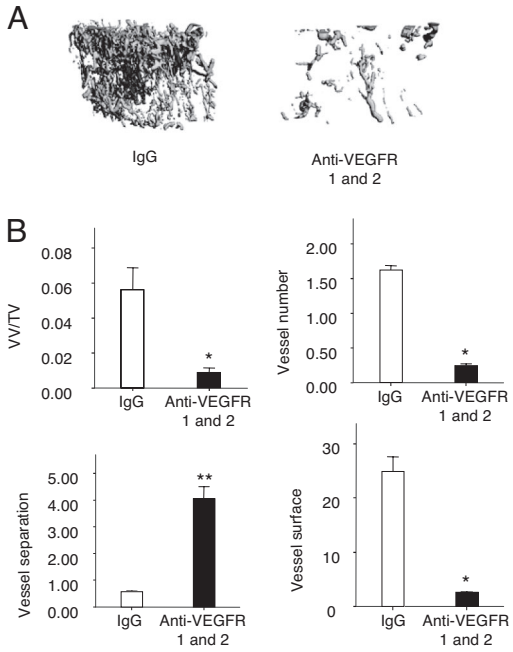

Fig. 2. VEGFR is required for neoangiogenesis during DO. Eight-week-old Δ*VHL* mice were injected i.p. with monoclonal antibodies against VEGFR-1 and -2 every 3 days after surgery for a total of five injections. Nonimmune IgG injection served as a negative control. At day 17 after surgery, mice were perfused with Microfil and analyzed for vessel formation in the distraction gap. (*A*) Representative μCT images of vasculature in Microfil-perfused distraction area are shown. (*B*) Quantitative measurements of vessel volume per total volume (VV/TV), vessel number, vessel separation, and vessel surface are shown. Data represent mean ± SD. *, $P < 0.05$, **, $P < 0.01$.

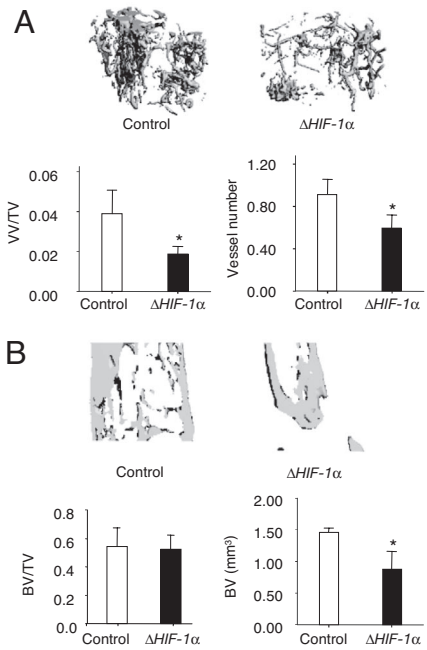

Fig. 3. Disruption of HIF-1α in osteoblasts impairs angiogenesis and bone regeneration during DO. (*A*) Representative μCT images of vasculature in Microfil-perfused distraction area from control and the Δ*HIF-1α* mice at day 17 after surgery. Quantitative measurements of vessel volume per total volume (VV/TV) and vessel number are shown. (*B*) Representative μCT images of distraction area from control and Δ*HIF-1α* mice at day 31 after surgery. Quantitative measurements of BV and BV/TV are shown. Data represent mean ± SD. *, $P < 0.05$.

ment with DFO, and to a lesser extent, L-mim, increased HIF-1α nuclear accumulation and VEGF mRNA expression in MSCs maintained under normoxic conditions (Fig. 4 *B* and *C*). We next tested DFO and L-mim for angiogenic activity using a standard Matrigel tube formation assay with human umbilical vein endothelial cells (HUVEC). Exposure to DFO and L-mim increased formation of tube-like structures (Fig. 4 *D* and *E*). To further evaluate the angiogenic activity of the PHD inhibitors, we performed an angiogenesis assay using explants of E17.5 mouse metatarsals. Control metatarsals exhibited a small degree of endothelial sprouting, which was greatly enhanced by treatment with rhVEGF in a time-dependent manner (Fig. 4*F* and SI Fig. 9). Continuous (14 days) exposure to DFO or L-mim was associated with detachment of the bone rudiments from the tissue culture plate, possibly because of the known effect of PHD inhibitors on collagen processing (17). However, exposure to DFO and, to a lesser degree, L-mim for a shorter period increased endothelial sprouting without obvious toxicity (Fig. 4*F*). Furthermore, treatment of mouse MSCs with these agents had no detectable effect on the ability of these cells to differentiate into osteoblasts *in vitro* as measured by alkaline phosphatase (ALP) staining (SI Fig. 10 and *SI Text*).

Because of the greater angiogenic activity of DFO *in vitro*, we selected it for evaluation *in vivo* in the DO model. DFO was administered directly into the distraction gap every other day over the period of active distraction from days 7 to 17. Separate experiments using methylene blue injections documented local delivery of the vehicle into the gap (Fig. 5*A*). DFO strongly increased vascularity in the distraction gap, as demonstrated by significantly increased vessel number and vessel connectivity at day 17 (Fig. 5 *B* and *D*). X-ray and μCT analysis at day 31 showed that bone regeneration was increased after DFO treatment. BV and BV/TV were significantly increased compared with controls. (Fig. 5 *A*, *C*, and *E*).

Discussion

In this article, we demonstrate that tissue hypoxia, which develops after a standard surgical distraction procedure in normal mice, is accompanied by up-regulation of the HIF/VEGF pathway and results in neoangiogenesis. We provide genetic evidence that the HIF-1 transcription factor is required to stimulate VEGF production and to mount a normal angiogenic and osteogenic response in a mouse model of bone repair. In addition, we provide proof of concept that this pathway can be targeted pharmacologically to augment bone regeneration.

Recent work from our laboratory and others have shown that *HIF-1* and its downstream target, *VEGF* are up-regulated in chondrocytes and osteoblasts within fracture callus (2, 18). VEGF has also been found in human fracture hematoma and serum after fracture (19, 20). Moreover, local application of VEGF has been used to enhance healing and angiogenesis in mouse, rat, and rabbit fracture and bone defect models (21–24). The present studies provide insights into the cellular and molecular mechanisms responsible for bone formation and repair. Neoangiogenesis is known to be required for bone to regenerate (25, 26), such that animal models with defective or delayed angiogenesis have impaired healing of DO (27). The current results show that activation of HIF-1α, either by genetic or pharmacologic means, leads to increased bone deposition proportional to the prior increase in vascularity. Therefore, the osteogenic process appears to be driven by angiogenesis, which is stimulated through HIF activation and VEGF production. Previous work has shown that VEGF is expressed by osteoblasts and undifferentiated cells within the distraction gap (28) and that *HIF-1α*, *VEGF-A*, *angiopoietin 1*, and *neuropilin* are induced with each episode of distraction during the DO process, suggesting the involvement of these pathways in the

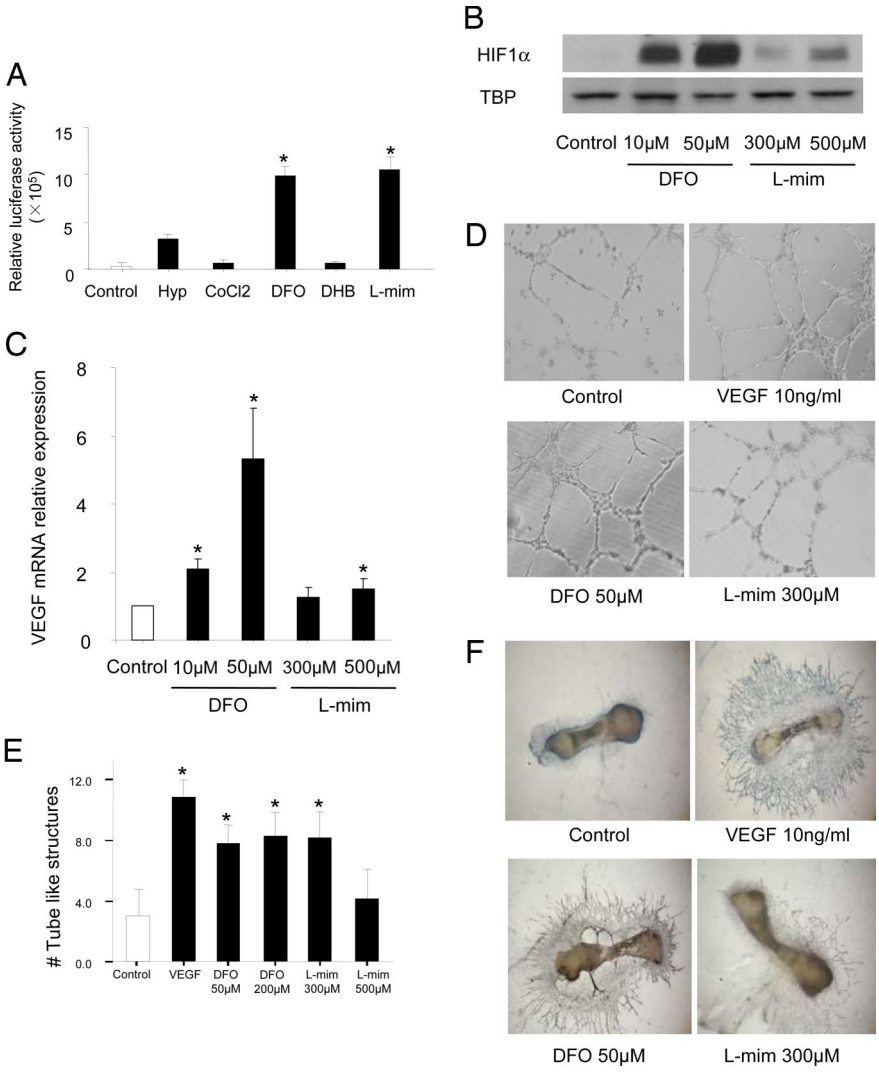

Fig. 4. Pharmacological activation of the HIF-1α pathway increases angiogenesis *in vitro*. (*A*) U2OS cells expressing an HRE reporter gene were exposed to hypoxia (Hyp) or treated with colbalt chloride ($CoCl_2$, 125 μM), DFO (200 μM), ethyl 3,4-dihydroxybenzoate (DHB, 700 μM), or L-mim (700 μM) under normoxia. Cells were harvested 24 h after treatment and analyzed for luciferase activity. (*B*) MSCs were collected from bone marrow of WT mice by using standard methods and cultured until confluent. Cells were untreated (control), or treated with DFO (10 and 50 μM) or L-mim (300 and 500 μM) under normoxia for 24 h. Nuclear protein was extracted from the cells and HIF-1α protein level was examined by immunoblotting analysis by using an anti-HIF-1α monoclonal antibody. Immunoblot for TBP (TATA box-binding protein) was used as loading control. (*C*) Total RNA was also extracted from cells, and VEGF mRNA expression was determined by using quantitative real-time PCR. Data represent mean ± SD. *, $P < 0.05$. (*D*) Matrigel tube-formation assay. HUVEC were cultured on Matrigel chambers with the addition of DFO (50 and 200 μM) or L-mim (300 and 500 μM) with VEGF (10 ng/ml) as positive control. Tube formation was photographed 12 h after treatment. (Magnification, ×100.) (*E*) Quantification of tube-formation assay by counting tube-like structure numbers. Data represent mean ± SD. *, $P < 0.05$. (*F*) *In vitro* metatarsal endothelial sprouting assay. Metatarsals were dissected from C57BL/6 E17.5 fetuses and cultured for 3 days for attachment. The explants were then cultured for another 6 days and then treated with DFO (50 μM) or L-mim (300 μM) for 24 h with rhVEGF (10 ng/ml) as positive control, followed by the detection of endothelial sprouting by immunostaining with anti-CD31 monoclonal antibody. Representative images are shown. (Magnification, ×25.)

angiogenic response (14). Furthermore, mechanical intervention induced by axial shortening after distraction resulted in improved healing in a rabbit DO model in association with HIF-1α upregulation, suggesting that the HIF pathway might also link mechanical stimuli to the regenerative response (29). However, although the VEGF pathway is important in mediating angiogenesis, VEGF alone was apparently insufficient to improve healing in a rabbit DO model (30). Thus, additional factors such as angiopoietins and Tie1 and 2 are likely required to restabilize endothelial cells after recruitment (31). Therefore, VEGF appears to be necessary, but not sufficient, to improve bone healing through angiogenesis in DO models. Because HIFs are upstream of the entire angiogenic cascade, they would be expected to induce additional factors required for reestablishing an intact vascular network in injured bone tissue. Although not specifically addressed in this study, it is likely that activation of the HIF pathway is also critical in other bone repair settings including those that require endochondral bone formation. Consequently, the HIF pathway is ideally suited for induction of angiogenesis in tissue repair and regeneration.

The precise mechanisms that couple angiogenesis to bone formation are still not known but appear to require cross-talk between osteoprogenitor cells and vascular endothelial cells. For example, the Δ*VHL* mice that overexpress *HIFs* and *VEGF* develop heavily vascularized long bones, yet when these *VEGF* overexpressing osteoblasts are cultured independently from blood vessels *in vitro*, they proliferate and differentiate similar to wild-type osteoblasts (13). This suggests that VEGF produced by the osteoblast stimulates neoangiogenesis in a cell nonautonomous fashion. Indeed capillaries are uniformly observed in bone modeling and remodeling compartments (32–34), and there is evidence that pericytes associated with the blood vessels may differentiate into osteoblasts (35). We propose that the angiogenesis observed in both developing (13) and regenerating bone (this study) would serve to increase the number of active bone (re)modeling units and provide a conduit for supply of circulating bone precursor cells and/or delivery of vessel-derived factors and cells required for bone formation.

The apparent requirement for angiogenesis in bone formation suggested the possibility that agents that stimulate angiogenesis might promote bone regeneration. In this study, we provide proof of principal that small molecules with HIF activating activity can be delivered into regenerating bone to augment healing. Previous work has identified a number of inhibitors of the prolyl hydroxylases that are required for ligation and proteosomal degradation of HIF (17, 36–40). The two agents used in this study, DFO and Lmim, inhibit PHDs through different mechanisms. DFO chelates iron, a cofactor required for enzyme activity, whereas L-mim is a competitive inhibitor of another cofactor 2-oxoglutarate. Both agents increased angiogenesis in standard HUVEC tube formation and fetal metatarsal endothelial sprouting assays *in vitro*. DFO significantly increased angiogenesis and bone formation in the DO model *in vivo*. Thus, in agreement with the genetic models of HIF

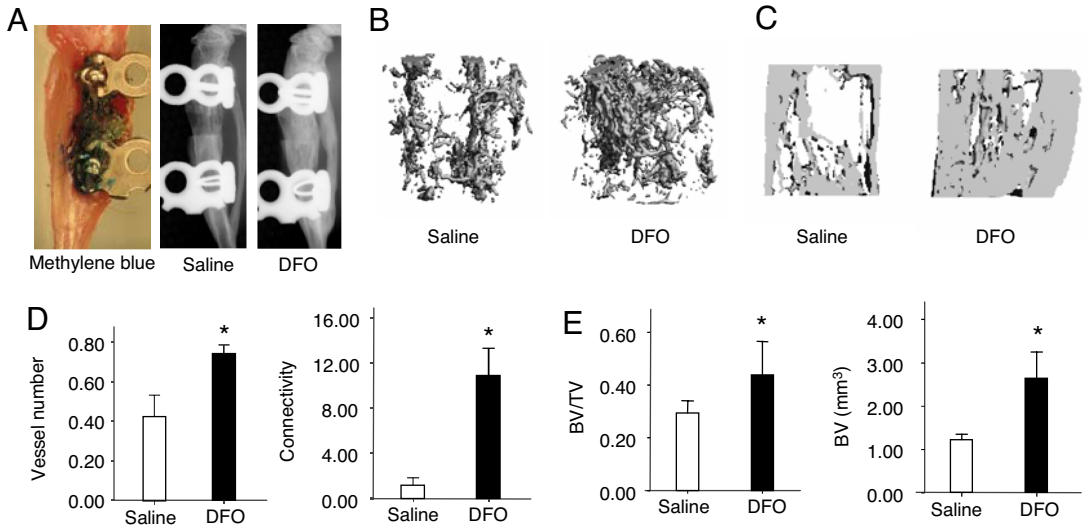

Fig. 5. Pharmacological activation of the HIF-1α pathway by DFO increases angiogenesis and promotes bone regeneration. Eight-week-old wild-type (C57BL/6) mice were subjected to DO. Mice were injected with DFO (200 μM) or saline as control in the distraction gap every other day from days 7 to 17 after surgery. (*A*) Validation of local injection approach using methylene blue following the same protocol with DFO treatment. X-ray images of control and DFO-treated mice at day 31 after surgery show bone regeneration in the distraction gap. (*B*) Representative μCT images of vasculature in Microfil-perfused distraction area from DFO-treated and control mice at day 17 after surgery. (*C*) Representative μCT images of distraction area from DFO-treated and control mice at day 31 after surgery. (*D*) Quantitative measurements of vessel number and connectivity are shown. Data represent mean ± SD. *, $P < 0.05$. (*E*) Quantitative measurements of BV and BV/TV are shown. Data represent mean ± SD. *, $P < 0.05$.

activation, pharmacologic stimulation of HIF activity also induced a robust angiogenic response that was coupled to a subsequent osteogenic response. However, in contrast to the genetic models in which *HIF-1α* was deleted in the osteoblast, direct delivery of DFO into the distraction gap would be expected to increase HIF activity in all cells including bone progenitors and endothelial cells. In this regard, the resultant new bone formation caused by DFO appeared to be even more robust than that seen in the genetic model, with evidence of new bone extending to all regions reached by the DFO solution. The overall efficacy and lack of overt toxicity of DFO is encouraging, given its potential to inhibit prolyl hydroxylation of collagen 1, and suggests some selectivity of this compound to target the HIF PHDs. Nonetheless, additional PHD inhibitors, custom peptides containing the HIF oxygen-degradation domain (ODD) (41) or transgenic constructs (42) are currently available and might represent useful alternatives to increase bone regeneration. The low cost and relative stability of PHD inhibitors are clearly advantageous and suggest promise as agents to improve blood supply to skeletal and other tissues that require angiogenesis to regenerate.

Materials and Methods

Generation of Conditional Knockout Mice. All procedures involving animals were in compliance with the guiding principles of the ''Care and Use of Animals,'' and approved by the University of Alabama at Birmingham Institutional Animal Care and Use Committee. Osteocalcin *Cre* (OC-*Cre*)-expressing mice (43) were crossed with mice homozygous for a floxed *VHL* allele (44) to obtain mice lacking pVHL, and therefore overexpressing HIFs in osteoblasts (OC-*Cre*;*VHL*$^{f/f}$). HIF-1α conditional knockout mice (OC-*Cre*; *HIF-1α*$^{f/f}$) were created by crossing OC-*Cre* mice with mice homozygous for a floxed *HIF-1α* allele (45). After appropriate breeding, OC-*Cre*;*VHL*$^{f/f}$ and OC-*Cre*; *HIF-1α*$^{f/f}$ mutant mice were generated. These mice have been described (13). PCR of DNA from tail biopsies was used to confirm the genotype.

Distraction Osteogenesis Model. DO was performed in the left tibiae of 8-week-old mice as described (14). Briefly, a modified 6-mm track distractor (KLS Martin) was attached to the tibia with 0.010-in ligature wire (3 M Unitek), and an osteotomy was performed with a saw. After 7 days of latency (no mechanical perturbation), distraction was performed at 0.15 mm/day for 10 days, for a total lengthening of 1.5 mm (days 7–17). Up to 21 days were then allowed for consolidation (days 18–38). Three pairs of mice were examined at the indicated time points for all DO experiments.

Radiographic Evaluation. Radiographs were performed by using a Faxitron x-ray machine. If the device changed position from its original placement or lost proper alignment during the experimental period, the animal was not used for any analysis. Computed tomography was used to quantify bone healing by using the μCT-40 system (Scanco Medical) and related analysis software. A volume of interest (VOI) was selected that contained the distraction osteogenesis area. Direct calculation of histomorphometric parameters was performed including BV, TV, BV/TV, bone surface (BS), trabecular thickness (Tb.Th), trabecular separation (Tb.Sp), and trabecular number (Tb.N). To evaluate the vascularity, μCT angiography was performed as described by Duvall *et al.* (46). At the end of the active distraction phase (day 17), the animals were euthanized and perfused with a radiopaque silicone rubber compound containing lead chromate (Microfil MV-122; Flow Tech). The distracted bones were removed, decalcified, and imaged by μCT. The VOI was defined as the distraction zone. Histomorphometric values including vessel volume, connectivity, number, thickness, and separation as well as degree of anisotropy were calculated.

Histology, Immunohistochemistry, and *in Situ* Hybridization Analysis. Tibae were also harvested, fixed, and decalcified with specimens embedded in paraffin for H&E staining, immunohistochemistry, and *in situ* hybridization. Immunostaining was performed per standard protocols after deparaffinization and rehydration. Sections were incubated with primary antibodies for pimonidazole (Hypoxyprobe-1) adducts (Millipore), HIF-1α (C-19; Santa Cruz Biotechnology), VEGF, CD31, and pVHL (BD Biosciences–Pharmingen). An HRP-Streptavidin detection system was used (Vector Laboratories). *In situ* hybridization was performed as described (45) by using complementary ^{35}S-labeled riboprobes for mouse VEGF mRNA.

Biomechanical Testing. Mice were euthanized at day 38, and tibiae were collected and fresh frozen. Specimens were tested to failure by three-point bending on 858 MiniBionix Materials Testing System (MTS Systems). Stiffness, peak load, and toughness were calculated from the force displacement data. Depth-control nanoindentation tests were performed on the same specimens by using a Nanoindenter XP (MTS Systems) with a Berkovich diamond indenter. Elastic modulus and hardness were calculated by established methods (47).

***In Vitro* Evaluation of Prolyl Hydroxylase Inhibitors.** A U2OS human osteosarcoma cell line stably expressing a luciferase reporter construct under the control of a hypoxia response element (U2OS-HRE-*luc*) (48) was used to quantify HIF

activation in response to commercially available agents described in published literature. U2OS-HRE-*luc* cells were treated for 24 h, and luciferase activity was detected by using the Bright-Glo luciferase reagent (Promega) and a luminometer. Cells cultured in hypoxia (1% O_2) served as positive controls.

Immunoblotting Analysis. Further *in vitro* evaluation of PHD inhibitors was performed by using MSCs isolated from marrow flushes of the femora and tibiae of WT mice. Ficoll column purification was performed, and the adherent cells were subcultured. Cells were exposed to DFO or L-mim for 24 h. Nuclear protein was extracted by using a NE-PER kit (Pierce). The extracts were separated on 10% SDS polyacrylamide gels and transferred to nitrocellulose membranes. After probing with primary antibodies, the membranes were incubated with HRP-linked secondary anti-rabbit antibodies (Cell Signaling Technology), and bound antibodies were visualized by using the Supersignal West Femto Maximum Sensitivity Substrate (Pierce). Antibodies used were anti-HIF-1α (R & D Systems) and anti-TATA box-binding protein (anti-TBP) (Abcam).

Quantitative Real-Time PCR. Total RNA was extracted by the TRIZOL protocol (Invitrogen). Real-time PCR was performed at 57°C for 30 cycles in the Opticon Continuous Fluorescent Detector by using IQTM SYBR green supermix (Bio-Rad). Triplicates were performed, and results were normalized to β-actin. We used the following primers: *VEGF-A*: F5′-*CCACGTCAGAGAGCAACATCA*-3′ and R5′-*TCATTCTCTCTATGTGCTGGCTTT*-3′.

***In Vitro* Angiogenesis Assays.** Effects on endothelial cells were evaluated by using a Matrigel tube formation assay (49). HUVEC were cultured on Matrigel chambers with the addition of DFO or L-mim with VEGF or VEGF antibody as positive and negative controls. Numbers of tube-like structures were counted after 12-h incubation. Metatarsal explant cultures were performed as described (50). Metatarsals from 17.5-day embryos were dissected and cultured in α-MEM with 10% FBS. Experimental bones were exposed to DFO or L-mim for 24 h, and medium was changed every 3 days. After 7 days, cultures were fixed and immunostained for CD31.

Administration of VEGFR Antibodies in DO Model. To evaluate whether effects seen in the Δ*VHL* mice were mediated by VEGF, mice were treated with monoclonal antibodies against mouse VEGF receptors [VEGFR-1 (clone mF-1) and VEGFR-2 (clone DC101) (ImClone Systems)]. I.p. injections were performed every 3 days after surgery for a total of five injections. Nonimmune IgG injection served as a negative control.

Administration of PHD Inhibitors in DO Model. For pharmacologic activation, C57BL/6 mice were injected with 20 μl of saline (control) or 200 μM DFO in the distraction gap every other day from days 7 to 17, for a total of five doses. To confirm correct placement of injection, methylene blue injections were also performed.

Statistical Analysis. Comparisons were made by using student's *t* test or Mann–Whitney test. Results were expressed as mean ± SD. Significance level used was $P < 0.05$.

ACKNOWLEDGMENTS. We thank Tim Nagy and Maria Johnson for support on μCT analysis, Shafiul Chowdhury for assistance with nanoindentation, Margaret Ashcroft (Institute of Cancer Research, Surrey, U.K.) for the U2OS-HRE-luc reporter cell line, Yabing Chen (University of Alabama at Birmingham) for providing HUVEC cells, and Cynthia Ballinger and Cheryl Perry for assistance in preparing the manuscript. This work was supported by National Institutes of Health Grants AR49410 (to T.L.C.), AR054771 (to S.R.G.), and P01-AR049920 (to L.C.G. and T.A.E.) and pilot Grant P30AR046031 through the University of Alabama Core Center for Basic Skeletal Research.

1. Einhorn TA (1995) *J Bone Joint Surg Am* 77:940–956.
2. Ferguson C, Alpern E, Miclau T, Helms JA (1999) *Mech Dev* 87:57–66.
3. Gerstenfeld LC, Cullinane DM, Barnes GL, Graves DT, Einhorn TA (2003) *J Cell Biochem* 88:873–884.
4. Ceradini DJ, Kulkarni AR, Callaghan MJ, Tepper OM, Bastidas N, Kleinman ME, Capla JM, Galiano RD, Levine JP, Gurtner GC (2004) *Nat Med* 10:858–864.
5. Cramer T, Yamanishi Y, Clausen BE, Forster I, Pawlinski R, Mackman N, Haase VH, Jaenisch R, Corr M, Nizet V, *et al.* (2003) *Cell* 112:645–657.
6. Robins JC, Akeno N, Mukherjee A, Dalal RR, Aronow BJ, Koopman P, Clemens TL (2005) *Bone* 37:313–322.
7. Yun Z, Maecker HL, Johnson RS, Giaccia AJ (2002) *Dev Cell* 2:331–341.
8. Kallio PJ, Wilson WJ, O'Brien S, Makino Y, Poellinger L (1999) *J Biol Chem* 274:6519–6525.
9. Ivan M, Kondo K, Yang H, Kim W, Valiando J, Ohh M, Salic A, Asara JM, Lane WS, Kaelin WG, Jr (2001) *Science* 292:464–468.
10. Maxwell PH, Wiesener MS, Chang GW, Clifford SC, Vaux EC, Cockman ME, Wykoff CC, Pugh CW, Maher ER, Ratcliffe PJ (1999) *Nature* 399:271–275.
11. Jaakkola P, Mole DR, Tian YM, Wilson MI, Gielbert J, Gaskell SJ, Kriegsheim A, Hebestreit HF, Mukherji M, Schofield CJ, *et al.* (2001) *Science* 292:468–472.
12. Kallio PJ, Okamoto K, O'Brien S, Carrero P, Makino Y, Tanaka H, Poellinger L (1998) *EMBO J* 17:6573–6586.
13. Wang Y, Wan C, Deng L, Liu X, Cao X, Gilbert SR, Bouxsein ML, Faugere MC, Guldberg RE, Gerstenfeld LC, *et al.* (2007) *J Clin Invest* 117:1616–1626.
14. Carvalho RS, Einhorn TA, Lehmann W, Edgar C, Al-Yamani A, Apazidis A, Pacicca D, Clemens TL, Gerstenfeld LC (2004) *Bone* 34:849–861.
15. Aronson J (1994) *Clin Orthop Relat Res* 124–131.
16. Choi IH, Ahn JH, Chung CY, Cho TJ (2000) *J Orthop Res* 18:698–705.
17. Nwogu JI, Geenen D, Bean M, Brenner MC, Huang X, Buttrick PM (2001) *Circulation* 104:2216–2221.
18. Komatsu DE, Hadjiargyrou M (2004) *Bone* 34:680–688.
19. Street J, Winter D, Wang JH, Wakai A, McGuinness A, Redmond HP (2000) *Clin Orthop Relat Res* 224–237.
20. Street JT, Wang JH, Wu QD, Wakai A, McGuinness A, Redmond HP (2001) *J Orthop Res* 19:1057–1066.
21. Eckardt H, Ding M, Lind M, Hansen ES, Christensen KS, Hvid I (2005) *J Bone Joint Surg Br* 87:1434–1438.
22. Geiger F, Bertram H, Berger I, Lorenz H, Wall O, Eckhardt C, Simank HG, Richter W (2005) *J Bone Miner Res* 20:2028–2035.
23. Peng H, Usas A, Olshanski A, Ho AM, Gearhart B, Cooper GM, Huard J (2005) *J Bone Miner Res* 20:2017–2027.
24. Street J, Bao M, deGuzman L, Bunting S, Peale FV, Jr, Ferrara N, Steinmetz H, Hoeffel J, Cleland JL, Daugherty A, *et al.* (2002) *Proc Natl Acad Sci USA* 99:9656–9661.
25. Ilizarov GA (1989) *Clin Orthop Relat Res* 263–285.
26. Ilizarov GA (1989) *Clin Orthop Relat Res* 249–281.
27. Choi P, Ogilvie C, Thompson Z, Miclau T, Helms JA (2004) *J Orthop Res* 22:1100–1107.
28. Pacicca DM, Patel N, Lee C, Salisbury K, Lehmann W, Carvalho R, Gerstenfeld LC, Einhorn TA (2003) *Bone* 33:889–898.
29. Mori S, Akagi M, Kikuyama A, Yasuda Y, Hamanishi C (2006) *J Orthop Res* 24:653–663.
30. Eckardt H, Bundgaard KG, Christensen KS, Lind M, Hansen ES, Hvid I (2003) *J Orthop Res* 21:335–340.
31. Yancopoulos GD, Davis S, Gale NW, Rudge JS, Wiegand SJ, Holash J (2000) *Nature* 407:242–248.
32. Khosla S, Eghbali-Fatourechi GZ (2006) *Ann NY Acad Sci* 1068:489–497.
33. Eriksen EF, Eghbali-Fatourechi GZ, Khosla S (2007) *J Bone Miner Res* 22:1–6.
34. Hauge EM, Qvesel D, Eriksen EF, Mosekilde L, Melsen F (2001) *J Bone Miner Res* 16:1575–1582.
35. Doherty MJ, Ashton BA, Walsh S, Beresford JN, Grant ME, Canfield AE (1998) *J Bone Miner Res* 13:828–838.
36. Bickel M, Baringhaus KH, Gerl M, Gunzler V, Kanta J, Schmidts L, Stapf M, Tschank G, Weidmann K, Werner U (1998) *Hepatology* 28:404–411.
37. Hermanns S, Reiprich P, Muller HW (2001) *J Neurosci Methods* 110:141–146.
38. Kim I, Mogford JE, Witschi C, Nafissi M, Mustoe TA (2003) *Wound Repair Regen* 11:368–372.
39. McCoy BJ, Diegelmann RF, Cohen IK (1980) *Proc Soc Exp Biol Med* 163:216–222.
40. Philipp S, Jurgensen JS, Fielitz J, Bernhardt WM, Weidemann A, Schiche A, Pilz B, Dietz R, Regitz-Zagrosek V, Eckardt KU, *et al.* (2006) *Eur J Heart Fail* 8:347–354.
41. Willam C, Masson N, Tian YM, Mahmood SA, Wilson MI, Bicknell R, Eckardt KU, Maxwell PH, Ratcliffe PJ, Pugh CW (2002) *Proc Natl Acad Sci USA* 99:10423–10428.
42. Huang LE, Gu J, Schau M, Bunn HF (1998) *Proc Natl Acad Sci USA* 95:7987–7992.
43. Zhang M, Xuan S, Bouxsein ML, von SD, Akeno N, Faugere MC, Malluche H, Zhao G, Rosen CJ, Efstratiadis A, *et al.* (2002) *J Biol Chem* 277:44005–44012.
44. Haase VH (2005) *Semin Cell Dev Biol* 16:564–574.
45. Schipani E, Ryan HE, Didrickson S, Kobayashi T, Knight M, Johnson RS (2001) *Genes Dev* 15:2865–2876.
46. Duvall CL, Taylor WR, Weiss D, Guldberg RE (2004) *Am J Physiol* 287:H302–H310.
47. Balooch G, Balooch M, Nalla RK, Schilling S, Filvaroff EH, Marshall GW, Marshall SJ, Ritchie RO, Derynck R, Alliston T (2005) *Proc Natl Acad Sci USA* 102:18813–18818.
48. Chau NM, Rogers P, Aherne W, Carroll V, Collins I, McDonald E, Workman P, Ashcroft M (2005) *Cancer Res* 65:4918–4928.
49. Ishida T, Kundu RK, Yang E, Hirata K, Ho YD, Quertermous T (2003) *J Biol Chem* 278:34598–34604.
50. Deckers M, van der Pluijm G, Dooijewaard S, Kroon M, van Hinsberg V, Papapoulos S, Lowik C (2001) *Lab Invest* 81:5–15.